Available online at www.sciencedirect.com
ScienceDirect
Science and Technology of Advanced Materials 8 (2007) 428–433
SCIENCE AND TECHNOLOGY OF ADVANCED MATERIALS
www.elsevier.com/locate/stam

Systematic study of the Grüneisen ratio near quantum critical points

R. Küchler, P. Gegenwart*, C. Geibel, F. Steglich

Max-Planck Institute for Chemical Physics of Solids, D-01187 Dresden, Germany

Received 6 March 2007; received in revised form 19 June 2007; accepted 21 June 2007
Available online 22 August 2007

Abstract

At any pressure-sensitive quantum critical point (QCP), the volume thermal expansion coefficient is more singular than the specific heat. Consequently, the resulting critical Grüneisen ratio $\Gamma^{cr}\sim\beta_{cr}/C_{cr}$, where β_{cr} and C_{cr} denote the thermal expansion and specific heat after subtraction of non-critical background contributions, diverges. The related critical exponent ε in $\Gamma^{cr}\sim T^{-\varepsilon}$ can be used to characterize the nature of the underlying quantum critical fluctuations. We have performed a comparative study on various heavy fermion (HF) systems close to antiferromagnetic QCPs. In particular, we have studied (i) $CeIn_{3-x}Sn_x$, (ii) $CeNi_2Ge_2$, (iii) $YbRh_2(Si_{0.95}Ge_{0.05})_2$, as well as (iv) $CeCu_{5.8}Ag_{0.2}$, all of which show a divergent Grüneisen ratio. For the two former systems the critical exponent $\varepsilon = 1$ is compatible with the predictions of the well-established Hertz–Millis–Moriya theory for three-dimensional extended quantum critical fluctuations. By contrast, for the two latter systems $\varepsilon < 1$ is found to be incompatible with "conventional" quantum criticality. Our results thus suggest the existence of at least two different classes of QCPs in HF systems.

Keywords: Critical point; Phase; Fluctuations; Temperature; Instability; Electron; Metals

1. Introduction

Heavy fermion (HF) systems, i.e. intermetallics of certain rare earths and actinides that contain a lattice of 4f- or 5f-derived moments, have turned out to be prototypical systems for the study of non-Fermi liquid (NFL) behavior [1]. Their ground-state behavior is determined by the competition between the on-site Kondo and the inter-site exchange interaction. When both interactions are balanced, a quantum critical point (QCP), separating a paramagnetic from a magnetically ordered ground state, occurs. The nature of quantum criticality in HF systems has been the focus of interest in recent years. Different scenarios for the QCP, where long-range antiferromagnetic (AF) order emerges from the HF state, have been proposed, e.g. a spin density wave (SDW) and a localized moment scenario. In the traditional SDW-picture [2–4], the quasiparticles retain their itinerant character when these materials are tuned into the long-range ordered state and, as a consequence, form an SDW-type of AF order. Recent experiments have shown that at least in some HF systems this picture fails [5,6]. Consequently, a new type of QCP has been proposed at which the quasiparticles break up into conduction electrons and local 4f moments, which order antiferromagnetically at sufficiently low temperatures. This picture has been labelled a "locally critical" scenario and is based on the destruction of the local Kondo resonances at the QCP [7,8].

In this paper, we give an overview on the use of measurements of the thermal expansion and critical Grüneisen ratio. While the Grüneisen parameter $\Gamma\sim\beta/C$, where C denotes the specific heat and β the volume thermal expansion, has long been used to describe the volume dependence of various physical processes [9], our results establish this quantity as highly suited to characterize QCPs. As a consequence of the entropy accumulation close to the zero-temperature instability, the critical Grüneisen ratio $\Gamma^{cr}(T)\sim\beta^{cr}(T)/C^{cr}(T)$ (here $\beta^{cr}(T)$ and $C^{cr}(T)$ denote the quantum critical contributions to the volume thermal expansion and the electronic specific heat, respectively) diverges in the approach of any pressure-sensitive QCP [10]. Within the SDW theory, the divergence is given by

*Corresponding author. Present address: First Physics Institute, Göttingen University, 37077 Göttingen, Germany.
E-mail address: kuechler@cpfs.mpg.de (R. Küchler).

1468-6996/$ - see front matter © 2007 Published by Elsevier Ltd.
doi:10.1016/j.stam.2007.06.010

$\Gamma^{cr} \sim 1/T^{1/\nu z}$ with the spatial correlation-length exponent ν and the dynamical exponent z. Measurements of the Grüneisen ratio are therefore apt to check the very existence of a QCP and to characterize its properties. In the following, we focus on $CeNi_2Ge_2$ [11], $CeIn_{3-x}Sn_x$ [12], $YbRh_2(Si_{0.95}Ge_{0.05})_2$ [6,13] and $CeCu_{5.8}Ag_{0.2}$ [14]. All four of them are well-characterized HF systems in the close vicinity of AF QCPs.

2. $CeNi_2Ge_2$

$CeNi_2Ge_2$ is a paramagnetic HF system with a single-ion Kondo scale of $T_K \approx 30$ K, crystallizing in the tetragonal $ThCr_2Si_2$ structure [15]. At zero magnetic field, pronounced NFL effects have been observed in thermodynamic and electrical transport experiments [11] related to a nearby magnetic instability. Indeed, substitution of Ni with the larger Pd in $Ce(Ni_{1-x}Pd_x)_2Ge_2$ induces long-range AF order below $T_N = 2$ K for $x = 0.2$ [16]. Furthermore, by applying magnetic fields, a Landau–Fermi liquid (LFL) state is induced with a coefficient $A(B)$, derived from the electrical resistivity $\Delta\rho = AT^2$, that diverges for $B \to 0$ [11]. Nevertheless, there are conflicting specific heat results about whether NFL behavior exists down to lowest temperatures or whether a cross-over to LFL behavior occurs. The earliest measurements show a small cusp in $C(T)/T$ at 0.3 K [15], while more recent work revealed a cross-over from a logarithmic increase above 0.3 K to a saturation at lower temperatures [17]. By contrast, $C(T)/T$ of a high-quality sample with very low residual resistivity does not saturate but shows an upturn at lowest temperatures [18]. We measured both the low-temperature volume thermal expansion, β, and specific heat, C, on high-quality single crystals with a residual resistivity of 5 μΩ cm. Fig. 1b displays the volume expansion coefficient β, plotted as $\beta(T)/T$. $\beta(T)$ has been calculated from the linear thermal

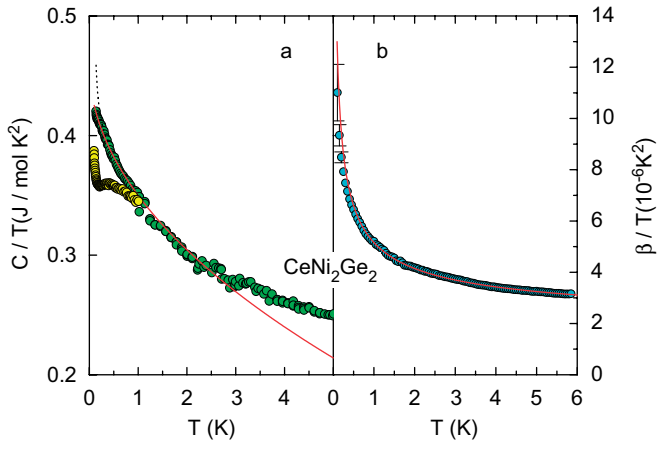

Fig. 1. Low-temperature specific heat as C/T vs. T (a) and volume thermal expansion as β/T vs. T (b) of a $CeNi_2Ge_2$ single crystal [29]. Red solid lines represent fits according to the 3D-SDW scenario. The dotted line in (a) represents the raw data, from which a contribution $C_n = a/T^3$ with $a = 102$ μJ K/mol has been subtracted. The yellow curve shows data at $B = 2$ T.

expansion coefficients of $CeNi_2Ge_2$ measured along the tetragonal a- and c-axis: $\beta = 2\alpha_a + \alpha_c$. $\beta(T)/T$ is not constant on cooling, as expected for an LFL, but shows a divergence over more than two decades in temperature from 6 K down to at least 50 mK. This clean observation of NFL behavior provides striking evidence that the single crystal is located very close to a QCP. As shown by the solid red line, the data can be described in the entire T range investigated by the temperature dependence predicted by the three-dimensional (3D)-SDW scenario [10], i.e. the sum of a singular ($\sim 1/\sqrt{T}$) and a normal (constant) contribution. The corresponding fit function is described by $\beta(T)/T = a/\sqrt{T} + b$, with $a = 3.5 \times 10^{-6}\,\mathrm{K}^{-1.5}$ and $b = 1.7 \times 10^{-6}\,\mathrm{K}^{-2}$. We now discuss the low-temperature specific heat (Fig. 1a) measured on the same sample. Below 3 K the electronic contribution of the specific heat could be described by $C(T)/T = \gamma_0 - c\sqrt{T}$ (red line), compatible with the 3D-SDW QCP scenario. Here we have assumed that the low-temperature upturn $C/T \sim a/T^3$ (dotted line), also present in this single crystal, is described by the high-temperature tail of a (nuclear) Schottky anomaly. However, the latter is yet unknown, since internal magnetic fields of the order of 30 T acting on the nuclear ^{61}Ni or ^{73}Ge spin states would be necessary to produce this contribution to our $B = 0$ data [18]. Of particular importance is the very fact that this upturn cannot be part of the quantum critical behavior: It remains unchanged in a magnetic field of about 2 T (yellow curve) that tunes the system toward the LFL regime. The influence of the low-T upturn in $C(T)/T$ on the Grüneisen ratio is smaller than 5% at 0.1 K and is, therefore, not visible in the $\Gamma(T)$ plot shown in Fig. 2. The observation of a divergent $\Gamma(T)$ for $T \to 0$ confirms a pressure-sensitive QCP in $CeNi_2Ge_2$ [10]. More generally, the results underline that the Grüneisen ratio provides a novel thermodynamic means of probing quantum phase transitions. To interpret our results, we discuss the exponent ε of the critical Grüneisen ratio $\Gamma^{cr} \propto 1/T^{\varepsilon}$. The observed quantum critical behavior of both the thermal expansion and specific heat in $CeNi_2Ge_2$ can be fit by $\beta^{cr} \propto \sqrt{T}$ and $C^{cr} \propto T^{3/2}$, respectively, leading to $\Gamma^{cr} \propto 1/T$. The Grüneisen exponent $\varepsilon = 1$ (with error bars $+0.05/-1$, as determined from the log–log plot shown in the inset of Fig. 2) is in full agreement with the 3D-SDW QCP prediction [10]. This is also compatible with results of inelastic neutron scattering (INS) experiments on $CeNi_2Ge_2$, which did not reveal any hint for quasi-2D magnetic fluctuations in this system [20].

3. $CeIn_{3-x}Sn_x$

Next, we focus on the HF system $CeIn_{3-x}Sn_x$, which crystallizes in the Cu_3Au structure with cubic point symmetry of the Ce-atoms (see inset of Fig. 3). It has been chosen for a detailed study, as here low-dimensional spin-fluctuations can be ruled out. Thus, the interesting question arises, whether the mechanism of NFL behavior in this system can be described by the itinerant 3D-SDW QCP

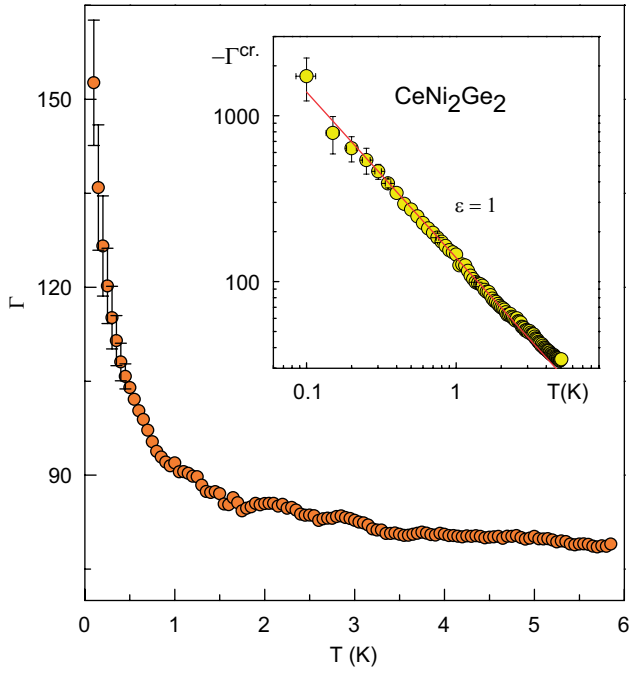

Fig. 2. Temperature dependence of the Grüneisen ratio $\Gamma = V_{mol}\,\kappa_T^{-1}\beta/C$ [29], where V_m and κ_T are the molar volume and isothermal compressibility, respectively. Since the latter has not been measured for $CeNi_2Ge_2$, we use $\kappa_T = 8.33\times10^{-12}\,Pa^{-1}$ obtained for the isostructural and related HF compound $CeCu_2Si_2$ [19]. The inset shows the critical component of Grüneisen ratio $\Gamma^{cr} = V_{mo}/\kappa_T^{-1}\beta^{cr}/C^{cr}$ as $\log\Gamma^{cr}$ vs. $\log T$ (at $B = 0$) with $\beta^{cr} = \beta(T) - bT$ and $C^{cr} = C(T) - (\gamma T + d/T)^2$. The solid red line represents $\beta^{cr} \propto 1/T^{\varepsilon}$ with $\varepsilon = 1$.

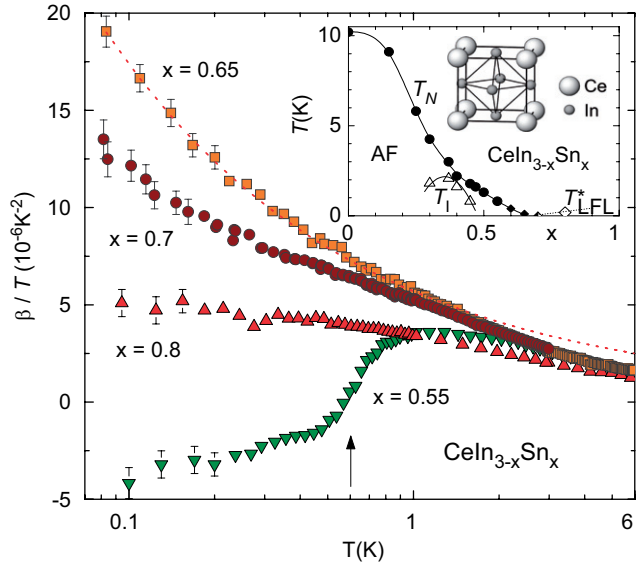

Fig. 3. Volume thermal expansion coefficient β of $CeIn_{3-x}Sn_x$ single crystals as β/T vs. $\log T$ [26]. The red dashed line shows $T^{-0.5}$ behavior. The arrow indicates AF phase transition. The inset shows the magnetic phase diagram for cubic $CeIn_{3-x}Sn_x$ ($x \leqslant 1$). Closed circles and diamonds indicate T_N, determined from specific heat [21] and electrical resistivity [22] measurements, respectively. Open diamonds marks T^*, the upper limit of Landau Fermi-liquid behavior, e.g. $\Delta\rho(T) \sim T^2$ [23]. Open triangles indicate the first-order transition T_I [21].

theory. The magnetic (x,T) phase diagram of polycrystalline $CeIn_{3-x}Sn_x$ has been thoroughly studied for $0 \leqslant x \leqslant 1$ by susceptibility [12], specific heat [21] and resistivity measurements [22,23] (see the inset of Fig. 3). Whereas T_N for undoped $CeIn_3$ vanishes abruptly below 3 K under hydrostatic pressure [24], it can be traced down to 0.1 K for $CeIn_{3-x}Sn_x$. These differences are related to the change of the electronic structure induced by Sn doping. Beyond a possible tetracritical point at $x \approx 0.4$ [21], an almost linear dependence of $T_N(x)$ is observed. Fig. 3 shows the volume thermal expansion β of single crystals of $CeIn_{3-x}Sn_x$ with $x = 0.55$, 0.65, 0.7 and 0.8 plotted as $\beta(T)/T$ vs. $\log T$. For $x = 0.55$ the broadened step-like decrease in $\beta(T)/T$ at $T_N \approx 0.6$ K marks the AF phase transition, in perfect agreement with specific heat measurements on the same single crystal [25]. On increasing the concentration, we find for $x = 0.65$ and 0.7 diverging behavior over nearly two decades in T down to 80 mK. These data suggest that T_N is suppressed at a critical concentration $x_c \approx 0.67 \pm 0.03$, also consistent with specific heat measurements performed on the same samples [25]. Finally, for $x = 0.8$ we recover LFL behavior, $\beta(T)/T \approx$ const. for $T \to 0$. According to the expression $\beta/T = a + bT^{\delta}$, the analysis of the $x = 0.65$ data reveals a fit of excellent quality (cf. the red dashed line in Fig. 3) for temperatures up to 1 K. The resulting exponent δ equals -0.5, i.e. the value predicted by the 3D-SDW QCP scenario [10] (for detailed analysis see [26]). Fig. 4 displays

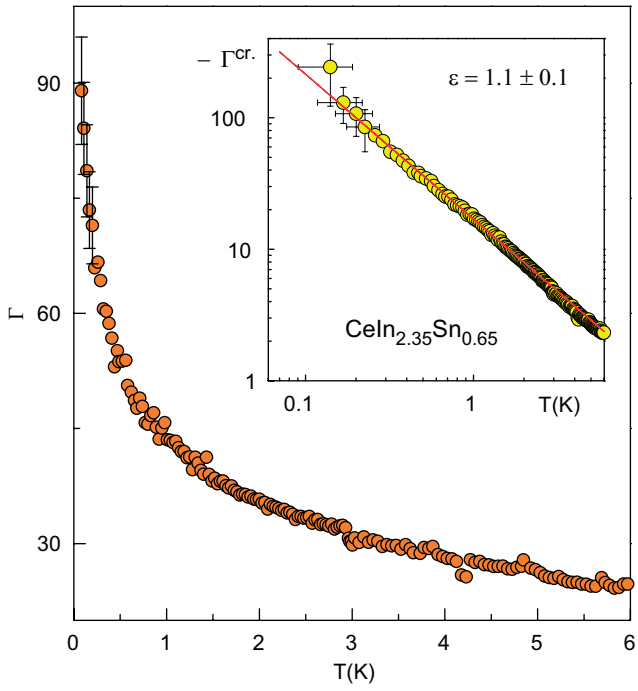

Fig. 4. Temperature dependence of the Grüneisen parameter $\Gamma = V_{mol}\kappa_T^{-1}\beta/C$ for $CeIn_{3-x}Sn_x$ ($x = 0.65$) [26]. $V_m = 6.25\times10^{-5}\,m^3mol^{-1}$ and $\kappa_T = 1.49\times10^{-11}\,Pa^{-1}$ [27] are the molar volume and isothermal compressibility, respectivly. The inset shows the critical component of the Grüneisen ratio $\Gamma^{cr} = V_{mo}/\kappa_T^{-1}\beta^{cr}/C^{cr}$ of the same single crystal as $\log\Gamma^{cr}$ vs. $\log T$ with $\beta^{cr} = \beta(T) - bT$ and $C^{cr} = C(T) - \gamma T$ derived after subtraction of background contributions (see text). The solid red line represents $\beta^{cr} \propto 1/T^{\varepsilon}$ with $\varepsilon = 1.1 \pm 0.1$.

the temperature dependence of the Grüneisen ratio $\Gamma(T)$ for the $x = 0.65$ sample calculated from the specific heat and thermal expansion measured on the same single crystal. Divergent behavior is observed down to the lowest accessible temperature with very large Γ values at 0.1 K, which are of similar size as those found for the other quantum critical HF systems discussed in this paper. The fact that the divergence of $\Gamma(T)$ in the quantum critical regime is stronger than logarithmic provides clear evidence for a pressure-sensitive QCP in the system. If the disorder present in the system would lead to a "smeared" quantum critical regime, $\Gamma(T)$ could diverge at most logarithmically [10]. In order to compare our results with the theoretical predictions for an SDW QCP [10], we analyze the critical Grüneisen ratio [26] that is displayed on double logarithmic scales in the inset of Fig. 4. We find $\Gamma^{cr} \sim T^{-\varepsilon}$ with an exponent close to 1, similar as for $CeNi_2Ge_2$, providing evidence for the applicability of the 3D itinerant theory in both systems.

4. $YbRh_2Si_2$

We now turn to $YbRh_2Si_2$, for which pronounced NFL behavior is observed above a weak AF ordering at $T_N = 70$ mK [13]. The ordering can be further weakened by a tiny volume expansion induced by the substitution of nominally 5 at% Ge for the smaller but isoelectronic Si in $YbRh_2(Si_{0.95}Ge_{0.05})_2$ [6]. Here, $T_N = 20$ mK, and a field-induced QCP occurs at a magnetic field of 0.027 T applied within the tetragonal plane. For temperatures above 50 mK, no effect of the AF transition is detected and the zero-field data above 50 mK do probe the true quantum critical behavior [6]. In $YbRh_2Si_2$, the volume thermal expansion coefficient $\beta(T)$ has a negative sign reflecting the decrease of the Kondo temperature with pressure, which is opposite as in the case of Ce-based HF systems. In Fig. 5, we compare the temperature dependence of the electronic specific heat C_{el}/T with that of the volume expansion coefficient β/T. At $T > 1$ K, $\beta(T)$ can be fit by $-T\log(T_0/T)$ with $T_0 \approx 13$ K (see the left solid black line in Fig. 5). At $T < 1$ K, the best fit is given by $a_1 + a_0 T$. Both fits are not only different from the expected 3D-SDW results discussed earlier, but also weaker than the $\log\log T$ form [10] expected in a 2D-SDW picture. The maximum at 20 mK in $C_{el}(T)/T$ marks the onset of very weak AF order [6]. This is suppressed by $B_c = 0.027$ T applied in the easy plane. At $B = B_c$, a power law divergence $C_{el}(T)/T \propto T^{-1/3}$ is observed for $T < 0.3$ K, which is clearly incompatible with the 2D-SDW picture [6]. At higher temperatures, the specific heat coefficient also varies logarithmically [6]. Because of the different slope compared with that of $\beta(T)/T$, the Grüneisen ratio is strongly temperature dependent above 1 K. Most importantly, below 1 K the critical Grüneisen ratio (see the inset of Fig. 5) diverges as $T^{-2/3}$, incompatible with the prediction of the SDW theory for an AF QCP. By contrast, such a fractional exponent would be consistent with the locally quantum critical picture [7,29]. Hall effect

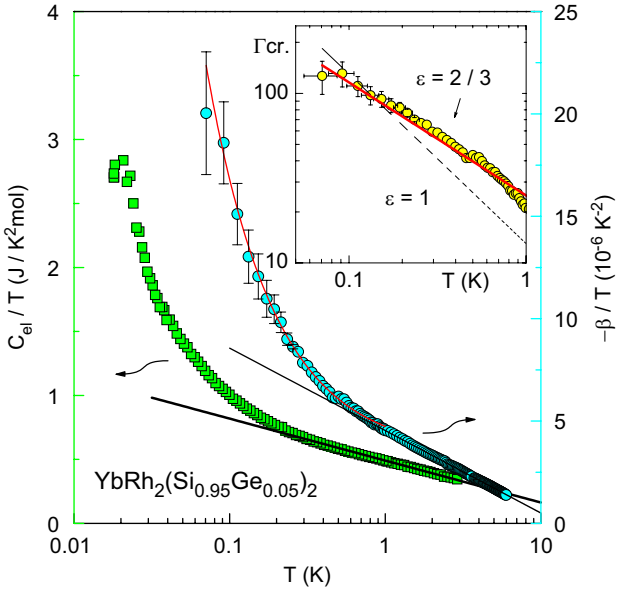

Fig. 5. Electronic specific heat as $C_{el}/T = (C - C_Q)/T$ (left axis) and volume thermal expansion as $-\beta/T$ (right axis) vs. T (on a logarithmic scale) for $YbRh_2(Si_{0.95}Ge_{0.05})_2$ at $B = 0$ [29]. Black solid lines indicate $\log(T_0/T)$ dependences with $T_0 = 30$ K and 13 K for C_{el}/T and $-\beta/T$, respectively. The red solid line represents $-\beta/T = a_0 + a_1/T$ with $a_0 = 3.4 \times 10^{-6}\,K^{-2}$ and $a_1 = 1.34 \times 10^{-6}\,K^{-1}$. The inset displays a double logarithmic plot of $\Gamma^{cr}(T)$ with $\Gamma^{cr} = V_{mol}/\kappa_T \beta^{cr}/C^{cr}$ using $\kappa_T = 5.3 \times 10^{-12}\,Pa^{-1}$ [28], $\beta^{cr} = \beta(T) + a_0 T$ and $C^{cr} = C_{el}(T)$. The solid red and the dotted black lines represent $\beta^{cr} \propto 1/T^{\varepsilon}$ with $\varepsilon = 0.7$ with $\varepsilon = 1$, respectively.

measurements have recently revealed a dramatic change of the Hall coefficient when tuning $YbRh_2Si_2$ across the QCP by varying the magnetic field [30]. This change is observed when crossing a scale $T^*(B)$ that merges at $T = 0$ at the critical field of 0.05 T. Thermodynamic measurements prove that $T^*(B)$ is an intrinsic energy scale (in the equilibrium spectrum) that vanishes at the QCP [31]. These results indicate that quantum criticality in $YbRh_2Si_2$ cannot be described within the conventional SDW theory. Unconventional quantum criticality with multiple vanishing energy scales seems to incorporate inherently quantum degrees of freedom that are not included in conventional order-parameter fluctuation theory.

5. $CeCu_{5.8}Ag_{0.2}$

Finally, we concentrate on the thermal expansion and critical Grüneisen ratio analysis of orthorhombic $CeCu_{5.8}Ag_{0.2}$. Our experiments are motivated by INS experiments on the related system $CeCu_{6-x}Au_x$, which have revealed an anomalous q-independence in the critical response and led to the proposal of a locally critical QCP scenario [5]. Fig. 6 displays the low-temperature specific heat divided by temperature, $C(T)/T$, of various $CeCu_{6-x}Ag_x$ samples on a logarithmic temperature scale [32]. Long-range AF order is observed for $x \geqslant 0.3$ and manifests itself by broadened jumps in $C(T)/T$. The inset shows $T_N(x)$ as determined by an (entropy-conserving)

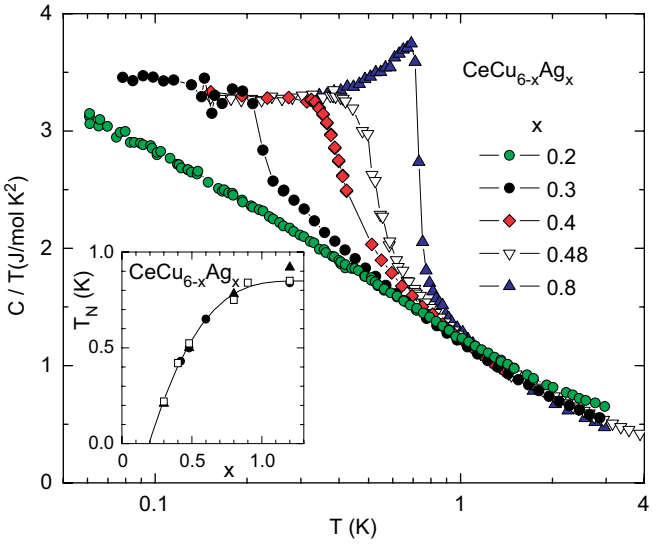

Fig. 6. Specific heat as C/T vs. T (on a logarithmic scale) for different $CeCu_{6-x}Ag_x$ polycrystals [38]. The inset shows the evolution of the antiferromagnetic phase transition temperature T_N vs. x as derived from specific heat (squares: this study, circles: [33]) and electrical resistivity [32]) results.

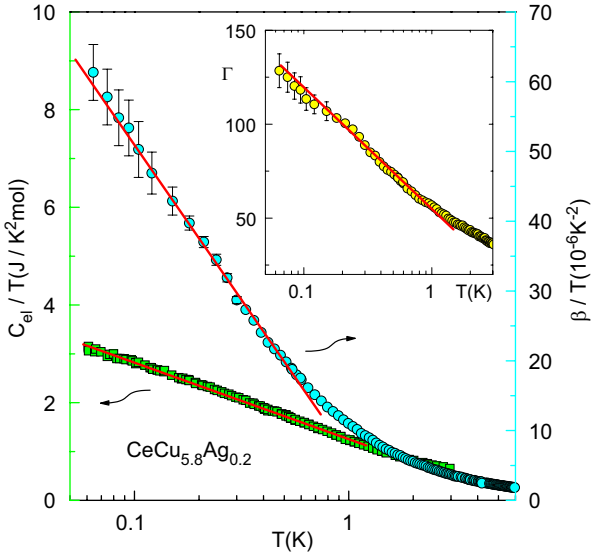

Fig. 7. Electronic specific heat as C_{el}/T vs. T (left axis) and volume thermal expansion as β/T (right axis) vs. T (on a logarithmic scale) for $CeCu_{5.8}Ag_{0.2}$ at $B = 0$ [38]. Red solid lines indicate log T dependences for C_{el}/T and β/T. The inset shows the temperature dependence of the Grüneisen parameter $\Gamma = V_m/\kappa_T^{-1}\beta/C$ with molar volume $V_m = 6.37 \times 10^{-5}\,m^3mol^{-1}$ and isothermal compressibility $\kappa_T = 1 \times 10^{-11}\,Pa^{-1}$ [37] on a logarithmic temperature scale. The solid red line represents a log(T) dependence.

equal-areas construction and the maximum of the derivative $d\rho(T)/dT$ in corresponding electrical resistivity measurements [32]. Extrapolation of T_N to zero temperature yields a critical concentration $x_c = 0.2$ (see the inset of Fig. 6). $CeCu_{5.8}Ag_{0.2}$ belongs to a class of $CeCu_6$-based HF systems in which the AF QCP is reached by doping the Cu-site [34,35]. Common to all of these systems is a universal $C/T \propto \log(T_0/T)$ dependence ($T_0 \approx 6$ K) of the specific heat coefficient over nearly two decades in temperature down to 50 mK (see the green curve in Fig. 6). This behavior would be compatible with theoretical predictions of the itinerant scenario for an AF QCP in the presence of 2D critical spin-fluctuations [10]. Indeed, INS experiments on $CeCu_{5.9}Au_{0.1}$ revealed rod-like structures of high intensity in q-space translating to quasi-2D fluctuations in real space [36]. The 2D-SDW picture, however, has been questioned by the observation of energy over temperature scaling in dynamical susceptibility with an anomalous fractional exponent, virtually independent of wave vector [5]. To further clarify the nature of QCP in this system, we now turn to thermal expansion, measured along three major perpendicular orientations, on the same polycrystal studied by specific heat (Fig. 7). The volume expansion coefficient β is determined by the sum of the three linear expansion coefficients α_i all showing a similar temperature dependence. On cooling to the lowest temperatures, $\beta(T)/T$ increases strongly and diverges logarithmically for $T \leqslant 0.8$ K (see Fig. 7). Although the observed $\beta(T)/T$ divergence is steeper than in C/T, indicating that NFL behavior is caused by a QCP, it is much weaker than the temperature dependence expected in the 2D-SDW scenario [10]. Finally, we discuss the temperature dependence of the Grüneisen ratio calculated from the specific heat and thermal expansion data shown in Fig. 7. In the entire temperature range, the divergence is weaker than $1/T$ and thus incompatible with the predictions of the itinerant scenario for both 3D or 2D critical spin-fluctuations [10].

6. Summary

To summarize, thermal expansion is more singular than specific heat in the approach of any pressure-sensitive QCP. The critical Grüneisen ratio of thermal expansion to specific heat is the most suitable thermodynamic property to characterize QCPs. The critical Grüneisen ratio diverges with an exponent that is directly related to the symmetry of the critical fluctuations. For the SDW theory, both in 3D and 2D, a $1/T$ divergence of the critical Grüneisen ratio is predicted. We have used a comparative study of the low-temperature thermal expansion and critical Grüneisen ratio to QCPs in the different HF systems. For cubic $CeIn_{3-x}Sn_x$ [26] and tetragonal $CeNi_2Ge_2$ [29] for which latter system INS measurements revealed 3D low-energy magnetic fluctuations [20], the critical Grüneisen ratio shows a $1/T$ divergence, in perfect agreement with the SDW scenario. By contrast, for $YbRh_2(Si_{0.95}Ge_{0.05})_2$ [29] and $CeCu_{5.8}Ag_{0.2}$ [38], a divergence with a significantly smaller exponent is observed, incompatible with SDW theory. On the other hand, there are indications for a more complicated structure of the critical magnetic fluctuations in both systems. For $CeCu_{5.9}Au_{0.1}$, closely related to $CeCu_{5.8}Ag_{0.2}$, INS has revealed quasi-2D critical fluctuations [36], while for $YbRh_2Si_2$ competing AF and ferromagnetic quantum critical fluctuations have been observed [39,40]. For these latter two systems, evidence for a locally critical QCP has

been found [5,6]. Our comparative study of the Grüneisen ratio divergence may thus suggest that a conventional AF QCP scenario, implying intact Kondo singlets and "composite" HFs at sufficiently low temperatures in the whole phase diagram, requires 3D critical spin-fluctuations.

Acknowledgments

Stimulating discussions with J.G. Sereni, Q. Si, M. Garst and L. Zhu are gratefully acknowledged. We thank O. Tegus, J.A. Mydosh, K. Heuser, G.R. Stewart, O. Stockert and N. Caroca-Canales for providing high-quality crystals and T. Cichorek, K. Neumaier, T. Radu and E.W. Scheidt for low-temperature specific heat measurements.

References

[1] G.R. Stewart, Rev. Mod. Phys. 73 (2001) 797.
[2] J.A. Hertz, Phys. Rev. B14 (1976) 1165.
[3] A.J. Millis, Phys. Rev. B48 (1993) 7183.
[4] T. Moriya, T. Takimoto, J. Phys. Soc. Jpn. 64 (1995) 960.
[5] A. Schröder, G. Aepli, R. Coldea, M. Adams, O. Stockert, H.V. Löhneysen, E. Bucher, R. Ramazashvili, P. Coleman, Nature 407 (2000) 351.
[6] J. Custers, P. Gegenwart, H. Wilhelm, K. Neumaier, Y. Tokiwa, O. Trovarelli, C. Geibel, F. Steglich, C. Pépin, P. Coleman, Nature 424 (2003) 524.
[7] Q. Si, S. Rabello, K. Ingersent, J.L. Smith, Nature (London) 413 (2001) 804.
[8] P. Coleman, C. Pépin, Q. Si, R. Ramazashvili, J. Phys. Condens. Matter 13 (2001) R723.
[9] E. Grüneisen, Ann. Phys. 39 (1912) 257.
[10] L. Zhu, M. Garst, A. Rosch, Q. Si, Phys. Rev. Lett. 91 (2003) 066404.
[11] P. Gegenwart, F. Kromer, M. Lang, G. Spam, C. Geibel, F. Steiglich, Phys. Rev. Lett. 82 (1999) 1293.
[12] J. Lawrence, Phys. Rev. B20 (1979) 3770.
[13] O. Trovarelli, C. Geibel, S. Mederle, C. Langhammer, F.M. Grosche, P. Gegenwart, M. Lang, G. Spam, F. Steiglich, Phys. Rev. Lett. 85 (2000) 626.
[14] K. Heuser, E.-W. Scheidt, T. Schreiner, G.R. Stewart, Phys. Rev. B 57 (1998) R4198.
[15] G. Knopp, A. Loidl, R. Caspary, U. Gottwick, C.D. Bredl, H. Spille, F. Steglich, A.P. Murani, J. Magn. Magn. Mater. 74 (1988) 341.
[16] G. Knebel, M. Brando, J. Hemberger, M. Nicklas, W. Trinkl, A. Loidl, Phys. Rev. B 59 (1999) 12390.
[17] S. Körne, A. Weber, J. Hemberger, E.-W. Scheidt, G.R. Stewart, J. Low Temp. Phys. 121 (2001) 105.
[18] F. Steglich, N. Sato, T. Tayama, T. Lühmann, C. Langhammer, P. Gegenwart, P. Hinze, C. Geibel, M. Lang, G. Sparn, W. Assmus, Physica C 341–348 (2000) 691.
[19] I.L. Spain, et al., Physica B + C 139 (1986) 449.
[20] H. Kadowaki, B. Fák, T. Fukuhara, K. Maezawa, K. Nakajima, M.A. Adams, S. Raymond, J. Flouquet, Phys. Rev. B 68 (2003) 140402.
[21] P. Pedrazzini, M.G. Berisso, N. Caroca-Canales, M. Deppe, C. Geibel, J.G. Sereni, Eur. Phys. J. B 38 (2004) 445.
[22] J. Custers, T. Cichorek, P. Gegenwart, N. Caroca-Canales, O. Stockert, C. Geibel, F. Steglich, P. Pedrazzini, J.G. Sereni, Acta Phys. Pol. B 34 (2003) 379.
[23] J. Custers, Ph.D. Thesis, Technische Universität Dresden, 2003 (unpublished).
[24] N.D. Mathur, F.M. Grosche, S.R. Julian, I.R. Walker, D.M. Freye, R.K.W. Haselwimmer, G.G. Lonzarich, Nature 394 (1998) 39.
[25] T. Rus, H. Wilhelm, O. Stockert, T. Lühmann, N. Caroca-Canales, J.G. Sereni, C. Geibel, F. Steglich, Physica B 359–361 (2005) 62.
[26] R. Küchler, P. Gegenwart, J. Custers, O. Stockert, N. Caroca-Canales, C. Geibel, J.G. Sereni, F. Steiglich, Phys. Rev. Lett. 96 (2006) 256403.
[27] I. Vedel, A.-M. Reden, J.-M. Mingot, J.-M. Leger, J. Phys. F: Met. Phys. 17 (1987) 849.
[28] J. Plessel, Dissertation, University of Cologne, 2001.
[29] R. Küchler, N. Oeschler, P. Gegenwart, T. Cichorek, K. Neumaier, O. Tegus, C. Geibel, J.A. Mydosh, F. Steglich, L. Zhu, Q. Si, Phys. Rev. Lett. 91 (2003) 066405.
[30] S. Paschen, T. Lühmann, S. Wirth, P. Gegenwart, O. Trovarelli, C. Geibel, F. Steglich, P. Coleman, Q. Si, Nature 432 (2004) 881.
[31] P. Gegenwart, et al., Science 315 (2007) 969–971.
[32] K. Heuser, Dissertation, University of Augsburg, 1999.
[33] G. Frauenberger, B. Andraka, J.S. Kim, U. Ahlheim, G.R. Stewart, Phys. Rev. B 40 (1989) 4735.
[34] H.V. Löhneysen, T. Pietrus, G. Portisch, H.G. Schlager, A. Schröder, M. Sieck, T. Trappmann, Phys. Rev. Lett. 72 (1994) 3262.
[35] M. Sieck, C. Speck, M. Waffenschmidt, S. Mock, H.V. Löhneysen, Physica B 223–224 (1996) 325.
[36] O. Stockert, H.v. Löhneysen, A. Rosch, M. Löwenhaupt, Phys. Rev. Lett. 80 (1998) 5627.
[37] G. Oomi, A. Shibata, Y. Onuki, T. Komatsubara, J. Phys. Soc. Jpn. 57 (1998) 152.
[38] R. Küchler, P. Gegenwart, K. Heuser, E.-W. Scheidt, G.R. Stewart, F. Steiglich, Phys. Rev. Lett. 93 (2004) 096402.
[39] K. Ishida, K. Okamoto, Y. Kawasaki, Y. Kitaoka, O. Trovarelli, C. Geibel, F. Steglich, Phys. Rev. Lett. 89 (2002) 107202.
[40] P. Gegenwart, J. Custers, Y. Tokiwa, C. Geibel, F. Steiglich, Phys. Rev. Lett. 94 (2005) 076402.